Malaysian Journal of Chemistry, 2025, Vol. 27(2), 75-87

Bio-based Polyurethane Foams from *Acacia mangium* Polyol: Analyzing the Impact of Polyol Residue, Surfactant, and Water on Foam Properties

Ismawati Palle[1]*, Naruhito Hori[2] and Akio Takemura[2]*
[1]Faculty of Tropical Forestry, Universiti Malaysia Sabah, Jalan UMS, 88400 Kota Kinabalu, Sabah, Malaysia
[2]Laboratory of Adhesive Science and Bio-composites, Department of Biomaterial Sciences, Graduate School of Agricultural and Life Sciences, The University of Tokyo, 1-1-1 Yayoi, Bunkyo-Ku, Tokyo, 113-8657, Japan
*Corresponding author (e-mail: isspalle@ums.edu.my; akiot@mail.ecc.u-tokyo.ac.jp)

This study investigated the synthesis of polyurethane foam using *Acacia mangium* (AM) polyol and its residue, with varying percentages of surfactant and water as blowing agents. The foam formulation included polymeric methylene bis(phenyl isocyanate) (pMDI), a catalyst mixture of triethylene diamine (TEDA-L33) and pentamethyldiethylene triamine (TOYOCAT-ET), polysiloxane (SH193) as the surfactant, and water as the blowing agent. The effect of incorporating AM polyol residue was first examined, followed by an analysis of the impact of the surfactant and blowing agent on the foam's properties, including kinetic rate, morphology, apparent density, water absorption, and compression behaviour. FTIR and DMA analyses were performed to assess the structural and mechanical properties of the foam. Results indicated that the addition of AM polyol residue significantly increased the foam density. However, reduced interfacial bonding between the residue and foam structure led to lower compression strength and higher water absorption. The study further showed that variations in water and surfactant content significantly influenced foam properties: increasing the water and surfactant content reduced foam density, accelerated the reaction between water and isocyanate (shortening the cream time), and enhanced nucleation and cell size. These findings suggest that AM polyurethane foam has potential as a sustainable alternative in industries seeking eco-friendly materials.

Keywords: Liquefied wood; 2D-COS analysis; blowing agent; FTIR

Received: October 2024; Accepted: February 2025

Polyurethane (PU) foams are polymers formed through the reaction of isocyanates with polyols, often supplemented by catalysts, blowing agents, surfactants, and other additives tailored for specific applications. These foams are widely used across various industries, including insulation, cushioning, packaging, and automotive components. Rigid polyurethane foams, in particular, are essential in the construction and insulation sectors, as they provide effective thermal insulation, which significantly reduces heating and cooling costs.

However, traditional PU foam production primarily relies on petroleum-based materials, raising significant environmental concerns. This dependence on non-renewable resources contributes to pollution and greenhouse gas emissions [1, 2, 3]. In response to these challenges, there is a growing shift towards bio-based polyols as sustainable alternatives. These not only reduce the reliance on fossil fuels but also align with the increasing demand for greener manufacturing practices in the foam industry.

The incorporation of bio-based polyols into PU foam production has emerged as a promising solution [4, 5, 6, 7, 8, 9]. Liquefied biomass, with its high hydroxyl content, has shown great potential as a polyol for PU foam formation. This high hydroxyl content enhances the polyol's reactivity with isocyanates, facilitating the formation of stable PU foams while promoting environmental sustainability. Among various bio-based polyols, *Acacia mangium* stands out as a particularly promising source due to its rapid growth rate and high hydroxyl content [10, 11]. Compared to other bio-based polyols, *A. mangium* polyol offers several unique benefits, including lower costs due to abundant availability, improved biodegradability, and potentially enhanced performance characteristics. These attributes make it an attractive option for sustainable foam production. Furthermore, the residue from *A. mangium* polyol, often underutilized, presents an additional opportunity to enhance the sustainability of PU foam production by reducing waste and lowering production costs.

Previous studies have demonstrated the potential use of bio-based fillers to improve PU foam properties. For example, the addition of biochar has been shown to enhance the dimensional and thermal stability of rigid PU foams [12]. A study by Członka et al. [13]

revealed that rigid PU composites reinforced with just 1 wt% coir-fibre filler exhibited significant improvements in physico-mechanical performance. These examples illustrate that bio-based fillers, including those derived from underutilized resources, hold significant potential for enhancing the properties of PU foams.

This study investigated the use of *A. mangium* polyol residue in bio-based PU foam formulations. Specifically, we explored how incorporating this residue can improve the mechanical properties of PU foams while reducing reliance on more conventional polyol sources. We also examined the role of blowing agents and surfactants. Water reacts with isocyanates to produce carbon dioxide (CO_2), which aids in foam expansion, while surfactants help stabilize the foam's cell structure and control its physical properties. We investigated how the incorporation *A. mangium* polyol residue, along with varying water loading and surfactant levels, influenced foam properties such as apparent density, compressive strength, water absorption, and viscoelastic behaviour. To characterize the resulting foams, techniques such as Fourier-transform infrared (FT-IR) spectroscopy and scanning electron microscopy (SEM) were employed. Given the high hydroxyl number of *A. mangium* polyol, a low NCO/OH ratio was preferred for optimal foam performance.

EXPERIMENTAL

Chemicals and Materials

The pMDI (polymeric methylene bis (*phenyl isocyanate*) MR 200 with NCO content of about 7.268 mmolg^{-1}, catalysts (triethylene diamine dissolved in dipropylene glycol to 33 wt %, TEDA-L33 and pentametyldiethylene triamine, TOYOCAT-ET) and polysiloxane (SH193) were supplied by TOSOH corporation, Yokohama, Japan. The 5 year old *A. mangium* wood chips supplied by Sabah Softwood Berhad (SSB), Sabah, Malaysia, were ground and sieved to obtain wood flour with a particle size of between 20-100 mesh (0.84 – 0.15 mm). Polyethylene glycol (#400), glycerol, sodium hydroxide, sodium chlorite and sulfuric acid were used as received.

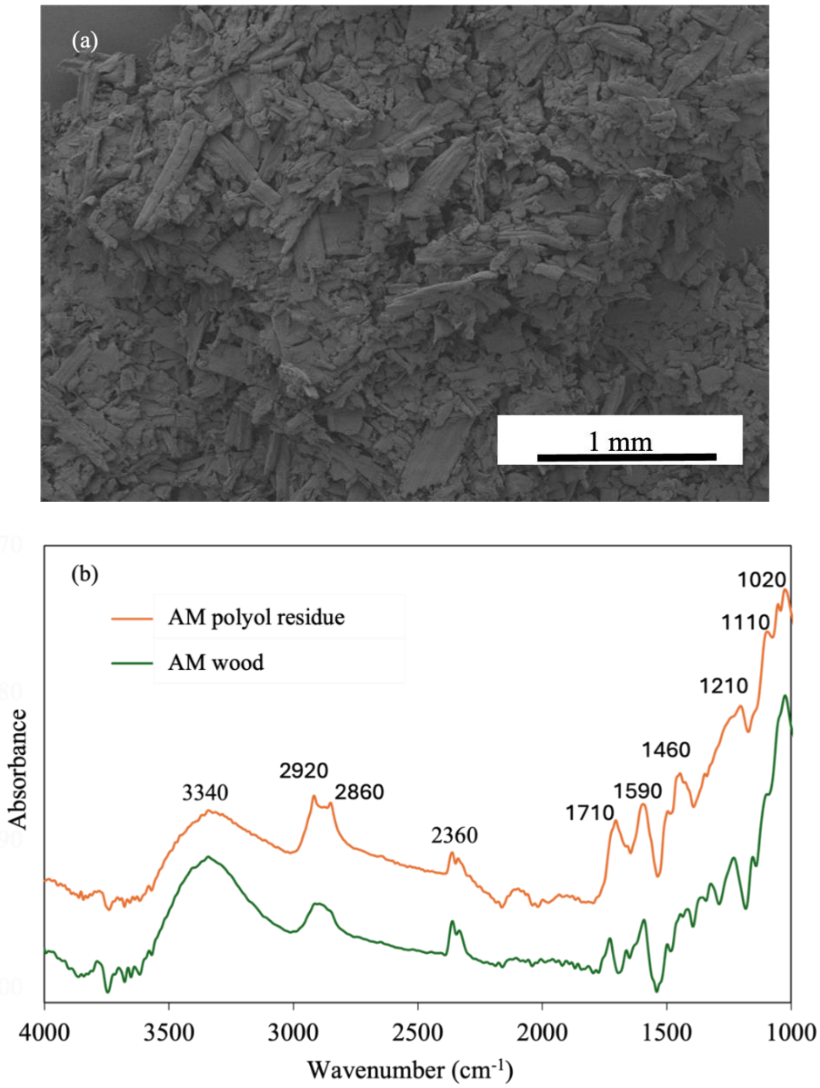

Figure 1. (a) SEM micrograph of AM polyol residue; (b) FTIR of AM wood and AM polyol residue.

Characterization Methods

Liquefaction of *A. mangium* Wood

The *A. mangium* polyol (AM polyol) was prepared as described in Palle et al. [11]. About 3 g of wood flour (20-100 mesh) was liquefied using a co-solvent mixture of polyethylene glycol and glycerol, with 3% H_2SO_4 as a catalyst, at a wood:liquor ratio of 1:3. The mixture was stirred and refluxed at 150 ºC for 150 min. After the reaction elapsed, the liquefied wood was diluted with methanol and filtered through Kiriyama filter paper (5C).

The filtrate obtained from this process was referred to as the AM polyol, while the material collected on the filter paper after filtration of the liquefied wood was referred to as the AM polyol residue. The AM polyol was then neutralized using 48 % NaOH [14] and filtered again to remove any remaining impurities. The AM polyol residue, which had particle sizes ranging from 10–50 µm (Figure 1a) and retained a chemical composition similar to pristine *A. mangium* wood (Figure 1b), was added back into the AM polyol after neutralization and filtration.

Finally, the mixture was stirred and evaporated at 45 ºC, followed by drying under vacuum at 80 ºC for 24 h. The water content of the AM polyol, including the polyol residue, was measured at 2 %, using a moisture analyzer (A&D Company, Limited).

Synthesis of *A. mangium* Polyurethane Foam

A. mangium polyurethane foam (AMPU foam) was prepared in two steps. Firstly, about 10 g AM polyol (hydroxyl number 438 mg KOH g^{-1}) (with and without residue), catalyst (TEDA L33 and TOYOCAT-ET) with a ratio of 4/1 (0.2 g), surfactant (SH193) (0.1-0.3 g) and water (blowing agent) (0.2-0.4 g) were premixed in a plastic cup and stirred with a glass rod for 60 s. Next, the predetermined pMDI was added and stirred for another 15 s by means of a mechanical stirrer at 1000 rpm. Three different types of AMPU foams were obtained, (1) with and without polyol residue, (2) with varying amounts of distilled water as blowing agent, and (3) with different percentages of polysiloxane (SH193) as surfactant, as detailed in Table 1. The schematic steps involved in the AMPU foam preparation are shown in Figure 2. The AMPU foam was allowed to rise in its plastic cup at room temperature for four days before being cut for analysis.

Table 1. Formulation of the AMPU foam.

AMPU foam	Residue (%)	NCO/OH ratio	Water (pbw)	Catalyst (pbw)	Surfactant (pbw)
AMPU-R	25	0.7	3	2	1
AMPU-WR	0	0.7	3	2	1
AMPU-2W	25	0.7	2	2	1
AMPU-3W	25	0.7	3	2	1
AMPU-4W	25	0.7	4	2	1
AMPU-1SH193	25	0.7	3	2	1
AMPU-2SH193	25	0.7	3	2	2
AMPU-3SH193	25	0.7	3	2	3

R (residue), WR (without residue), W (water), SH193 (surfactant), pbw (part by weight)

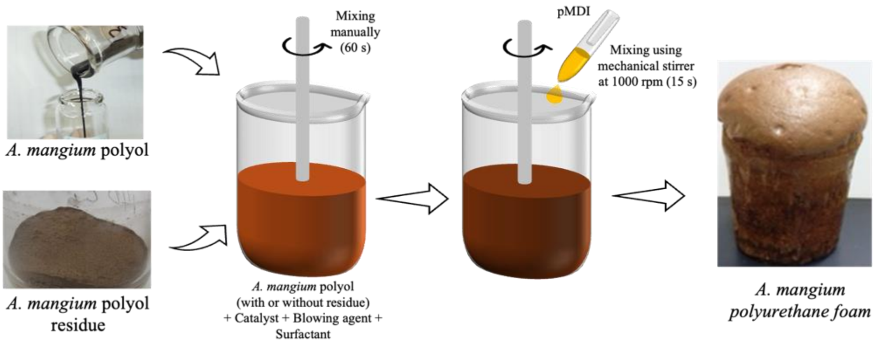

Figure 2. Schematic procedure of AMPU foam preparation.

Characterization of *A. mangium* Polyurethane Foam

The AMPU foams were characterized by Fourier Transform Infrared (FTIR) analysis using the KBR pellet method. About 2 mg of foam powder were mixed with 200 mg KBR to form a pellet. The data was analyzed using a Thermo Scientific Nicolet 6700 FTIR Spectrometer in the range of 4000-500 cm^{-1}. A total of 128 scans were accumulated at 4 cm^{-1} resolution. To evaluate the effect of the parameters studied on the AMPU foam functional groups, the absorbance peak at 2946 cm^{-1} was used as the standardized peak. 2D-COS IR spectroscopy was used in characterizing structural changes in AMPU foams at the carbonyl region as a function of different water loadings. The resulting spectra were evaluated by the 2DShige Software (2D shige (c) Shigeaki Morita, Kwansei Gakuin University, 2004-2005).

The sample viscosity was measured using Thermo Scientific HAAKE Rheo Stress 600 (20±0.1 °C).

The kinetic rate of the AMPU foam was determined according to ASTM D7487. The foaming characteristics were observed, and the time was recorded when the foam rose completely and lost its tackiness.

The sample morphology was verified by scanning electron microscopy (SEM) using the SEM 4800 (Hitachi, Japan) instrument at 1.0kV accelerating voltage. Before the test, the prepared specimens were sputter-coated with a thin layer of gold under a vacuum environment.

The apparent density of the AMPU foam was calculated from the mass and volume of the foam. The specimen size was 20 x 20 x 20 mm. The density values obtained were averaged from four specimens.

Compression properties of the AMPU foam were measured using the EZ-S Shimadzu 100N, Trapezium software at a crosshead speed of 5.0 mm min^{-1} with sample dimensions of 20 x 20 x 20 mm. The compressive moduli of the foams were determined based on the maximum modulus of elasticity.

Water absorption properties of the AMPU foam were measured based on the percentage by weight of samples that were air-dried after being immersed in water for 24 h. The size of each specimen was 20 x 20 x 20 mm and the average of four samples was taken.

The dynamic mechanical analysis (DMA) as a function of temperature was performed at the frequency of 10 Hz between -150 ºC and 250 ºC with a heating rate of 10 ºC min^{-1} using ITK DMA (Osaka, Japan). For the square test specimen, a thickness of 4-5 mm was prepared. The properties were measured parallel to the foaming direction.

Statistical Analysis

The experiments were replicated four times, and an analysis of variance (ANOVA) was conducted to evaluate the effects of residue, surfactant and blowing agent on the apparent density, water absorption, and compression strength of the AMPU Foam. The analysis was performed using SAS statistical software. Post-hoc comparisons were then carried out using the Least Significant Difference (LSD) test, with a significance level of $p \leq 0.05$.

RESULTS AND DISCUSSION

FTIR Analysis

FTIR spectra of the AMPU foams with and without residue, different water loadings and different surfactant percentages are presented in Figure 3a-c. The peaks indicative of urethane linkages were observed at 3320 cm^{-1} (N-H stretching), 1720 cm^{-1} (C=O stretching), 1540 cm^{-1} (amide II) and 1230 cm^{-1} (amide III) [15, 16, 17, 18, 19]. Notably, the free isocyanate peak (2270 cm^{-1}) almost entirely disappeared in the AMPU foam without residue. In contrast, this peak remained unchanged at higher surfactant loadings, while the amide linkages at 1730 cm^{-1}, 1510 cm^{-1}, and 1409 cm^{-1} increased significantly (Figure 3b). This suggests that surfactants enhanced the reaction between isocyanates and the hydroxyl groups of the residue, leading to an increase in amide groups. For varying water loadings, the amine linkages at 3320 cm^{-1} and amide groups also increased, confirming enhanced reactions between water and isocyanate (Figure 3c). The absence of the 2270 cm^{-1} band for 2 parts by weight (pbw) water loading indicated the complete reaction of all isocyanate groups. A shoulder peak at 1660 cm^{-1}, attributed to C=O urea formation, also increased with water loading [10, 19]. Higher water loading facilitates the reaction between free isocyanate and amine, promoting urea formation.

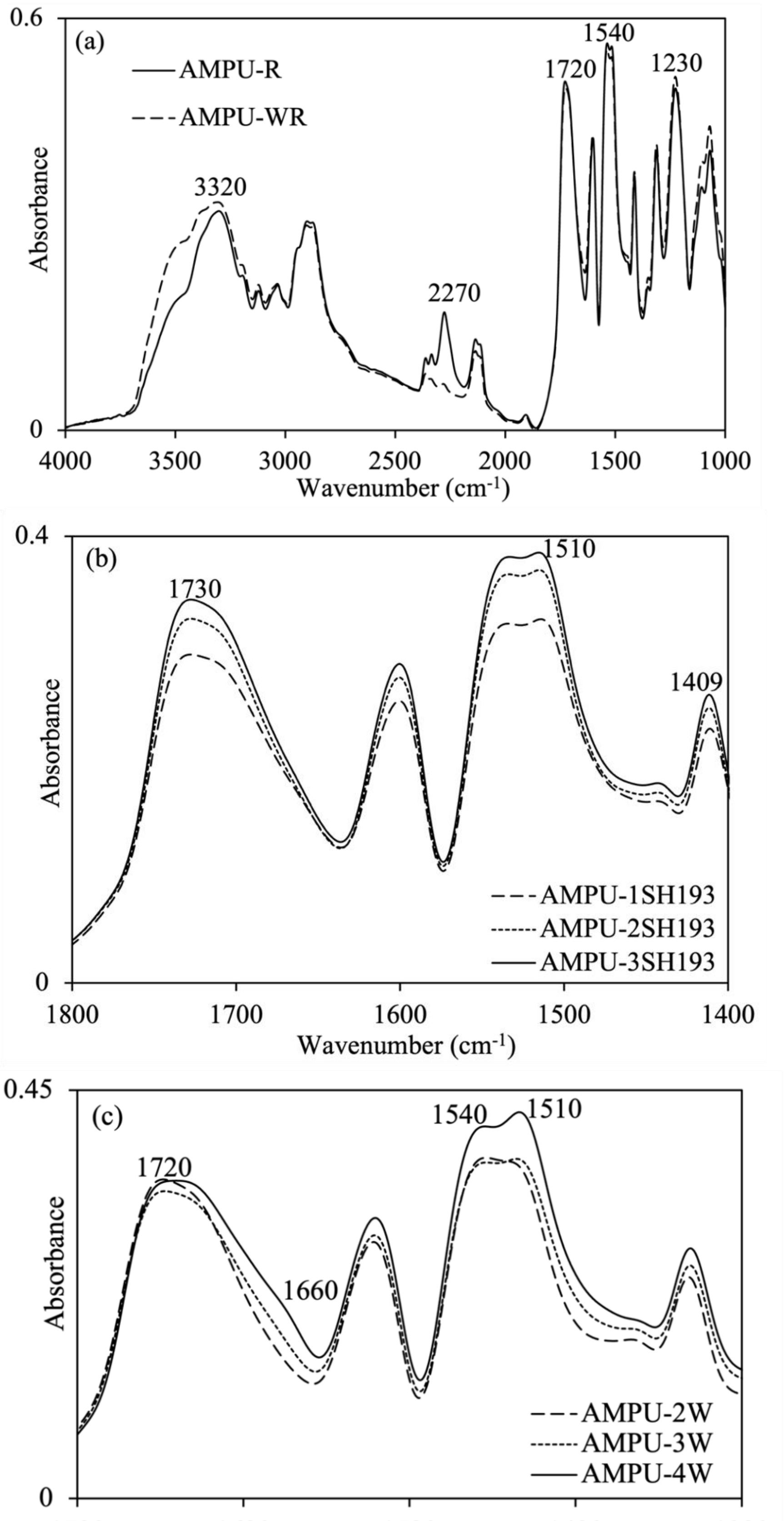

Figure 3. FTIR spectra of AMPU foams (a) with residue (AMPU-R) and without residue (AMPU-WR), (b) with different surfactant loadings, and (c) with different water loadings, in the amide region.

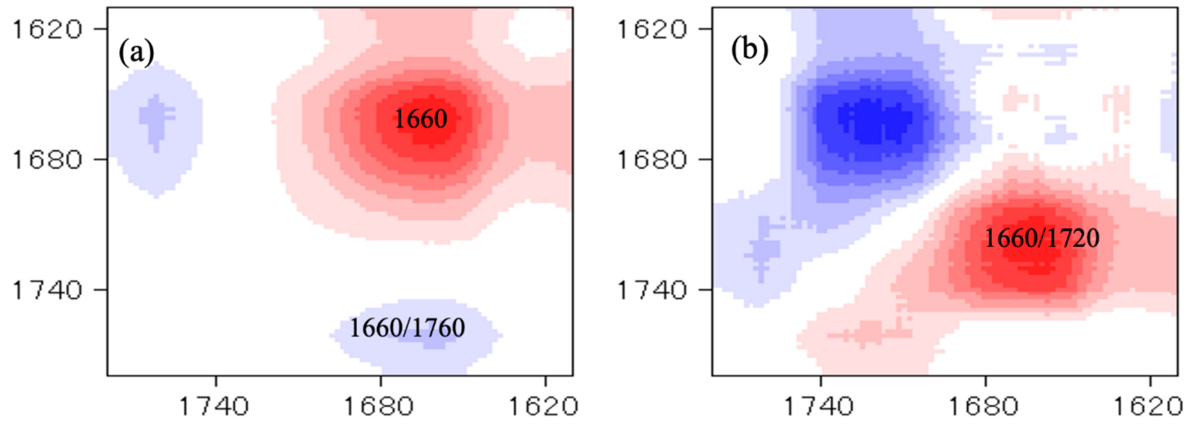

Figure 4. (a) Synchronous and (b) asynchronous spectra of AMPU foams at different water loadings.

Table 2. Kinetic rates of AMPU foams.

AMPU Foam	Kinetic rate		
	Cream time (s)	Rise time (s)	Tack time (s)
AMPU-R	10	35	210
AMPU-WR	16	56	249
AMPU-2W	30	75	274
AMPU-3W	16	56	249
AMPU-4W	<3	44	214
AMPU-1SH193	16	56	249
AMPU-2SH193	10	44	213
AMPU-3SH193	7	43	203

R (residue), WR (without residue), W (water), SH193 (surfactant)

To analyze the sequence of reactions during AMPU foam formation at different water loadings, we employed the 2D-COS technique to study correlations among functional groups in the carbonyl region. The synchronous spectrum (Figure 4a) revealed a strong auto-peak at 1660 cm^{-1}, indicating its sensitivity to increased water loading. A negative cross-peak between 1660/1760 cm^{-1} suggests that these bands changed directionally with increasing water loading. The asynchronous spectrum (Figure 4b) showed positive signs for 1660/1720 cm^{-1}, indicating that urea formation occurred before urethane formation, suggesting a first-order reaction. The disappearance of the 1660/1760 cm^{-1} bands in the asynchronous spectrum implied that these reactions occurred concurrently [20].

Kinetic Rate and Morphology

The synthesis of AMPU foams involved measuring critical kinetic rates, including cream time, rise time, and tack time (Table 2). Both cream time (the duration for the mixture to achieve a creamy consistency) and rise time (the period for the mixture to reach its maximum height) were considerably longer for foams containing residue (56 s) compared to those without residue (35 s). This delay was likely due to the apparent viscosity of AM polyol with residue (1.146 Pa•s), which was threefold higher than that of the polyol without residue (0.425 Pa•s). According to Szycher [21], increased viscosity hinders the mixing process with pMDI, leading to less uniform foaming and longer gelling times. Additionally, the high viscosity restricts foam expansion, leading to denser foams, as observed in the SEM images (Figure 5b), which showed smaller cell sizes in foams with residue. Rodrigue et al. [22] suggested that a higher concentration of wood particles promotes nucleation, restricts cell growth and results in smaller cell sizes. Furthermore, the reactive functional groups of the polyol residue may interact with isocyanate groups, disrupting the stoichiometric balance of the reaction and hindering the release of blowing agents (CO_2). This chemical disruption further limits foam expansion as more particles are incorporated into the PU polymer matrix [8, 13].

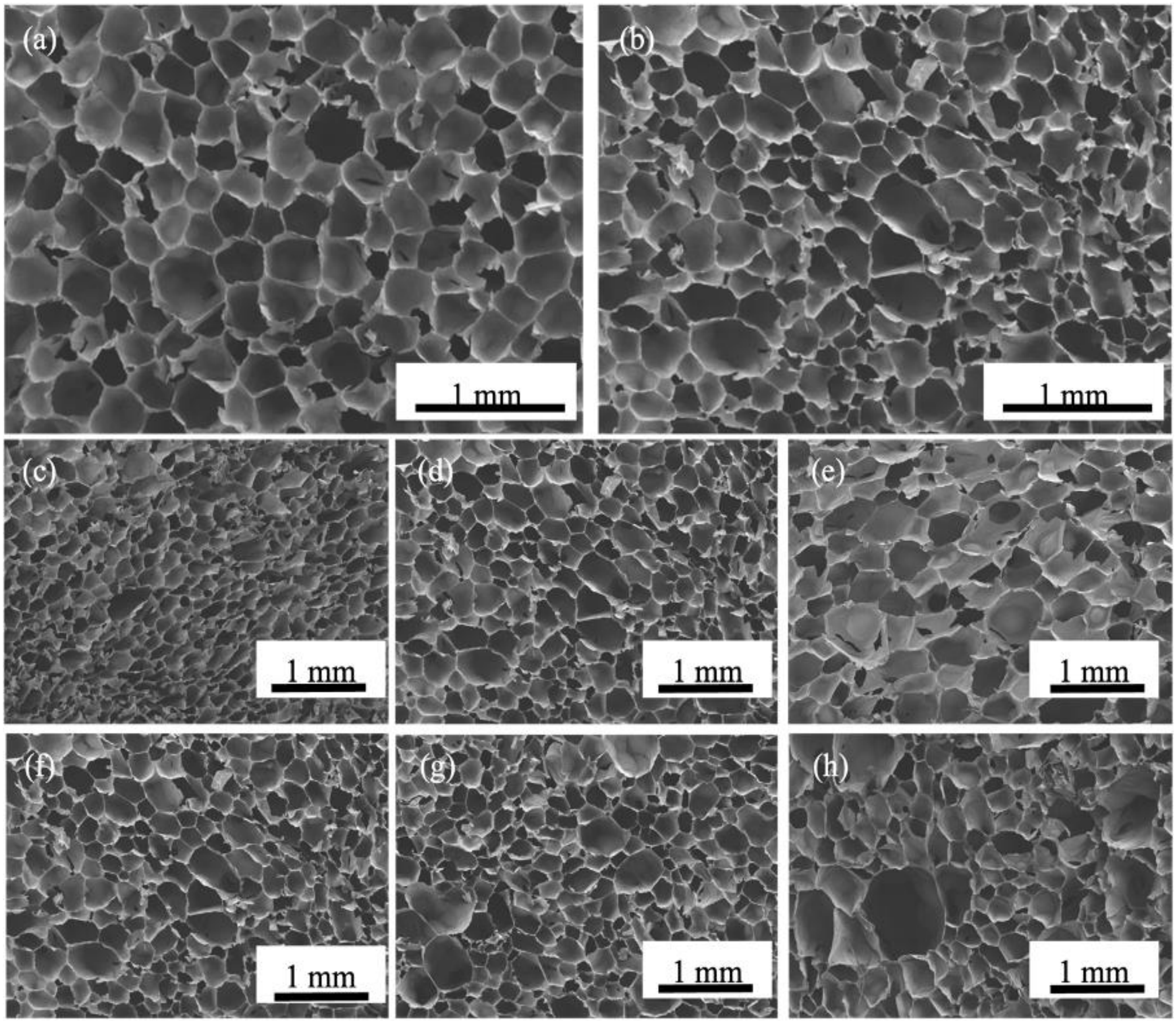

Figure 5. SEM micrographs of AMPU foams (a) without residue (AMPU-WR) and (b) with residue (AMPU-R); (c-e) different water loadings, 1-3 pbw; (f-h) different surfactant loadings,1-3 pbw.

In contrast, 4 pbw water loading exhibited a significantly shorter cream time of less than 3 s. An increased water content enhanced the reaction between isocyanate and water, producing more CO_2 [23, 24] and accelerating foam expansion. This rapid gas generation led to a lower foam density. Niyogi et al. [24] described the first-order reaction between water and isocyanate, indicating that increased water loading speeds up the blowing reaction relative to gelling. SEM images (Figure 5c-e) revealed larger cell sizes with higher water content. Increased water concentrations led to enhanced gas formation and reduced solubility limits, resulting in larger bubbles [25].

High surfactant loading correlated with increased cream and rise times (Table 2). The improved flowability from the high surfactant content effectively separated bubbles from the cell membrane, transforming them into polyhedral shapes (Figure 5f-h). The exothermic nature of the reaction caused phase separation into gas, leading to bubble growth and coalescence. While high surfactant concentrations typically promote finer and more uniform cell structures due to reduced surface tension, excessive surfactant can lead to self-aggregation, resulting in larger cell sizes due to coalescence [26].

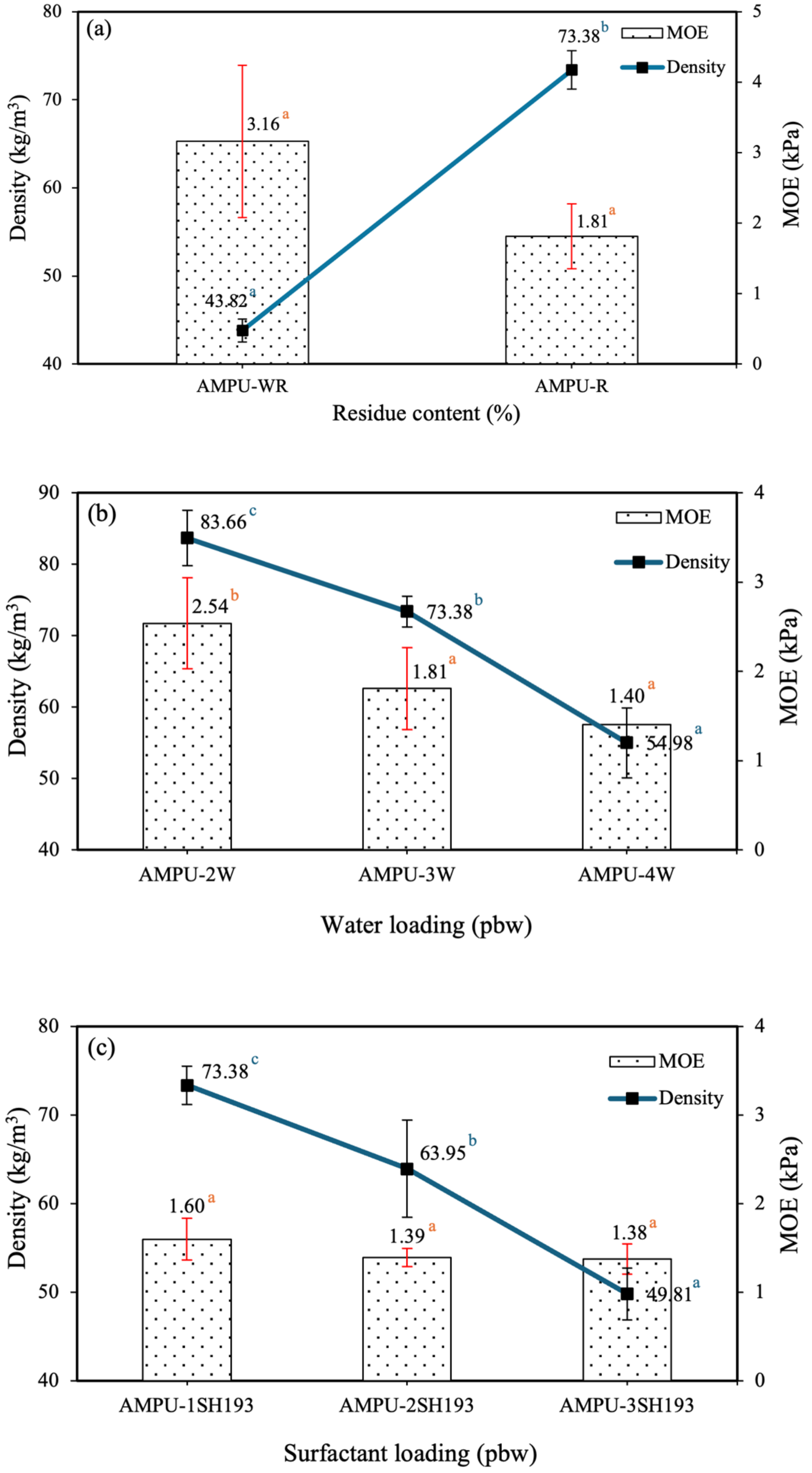

Figure 6. Density and compression properties MOE (kPa) of AMPU foam: (a) with residue (AMPU-R) and without residue (AMPU-WR), (b) with different water loadings, (c) with different surfactant loadings.

Apparent Density and Compression Properties

In foam composites, density is a critical parameter that affects the mechanical properties of the foam. Introducing AM polyol residue significantly increased foam density (Figure 6a). The density of the foam without residue was approximately 43.82 kg/m³, and this increased by 67 % when the residue was added, primarily due to the its high bulk density. However, while the residue enhanced the foam's density, it also reduced its elasticity, with the compressive modulus decreasing from 3.16 MPa (for foams without residue) to 1.81 MPa (Figure 6a). Typically, increased density correlates with a higher compressive modulus due to closer polymer chain packing. However, this trend was disrupted by the incorporation of residues, consistent with previous studies [25, 27, 28] which found that the incorporation of wood flour also led to reduced compressive strength. Krishnamurthi et al. [29] and Borreguero et al. [27] suggested that high blowing reactions can create voids in the foam, where agglomerated residues hinder stress transfer between membrane cells, resulting in structural deficiencies and lower compression properties.

Increasing the water loading significantly decreased the foam density from 83 kg/m³ to 55 kg/m³ (Figure 6b). Niyogi et al. [24] attributed this reduction to the accelerated reaction between water and isocyanate, which speeds up the blowing process. High water content leads to rapid CO_2 generation, causing supersaturation and shortening the nucleation period, which in turn promotes foam expansion and lowers the density. The compressive modulus of the foam also decreased with higher water loading, consistent with previous studies [28]. Goods et al. [30] explained that in closed-cell foams, stiffness is influenced by strut bending, membrane stretching, and internal gas pressure. Rapid CO_2 diffusion can create negative pressure gradients, leading to cell deformation [21, 25]. Larger cell sizes with thinner walls (Figure 5e) are expected to contribute to lower elasticity, as these structures are less capable of withstanding stress.

Increasing surfactant loading significantly reduced foam density, which is consistent with the findings of Lim et al. [1], who observed similar effects with silicon surfactants (B 8404) in their foam formulations. Higher surfactant content improved emulsification and accelerated the reaction mixture [21]. Surfactants facilitated the formation of nuclei and enhanced the emulsification of incompatible components, leading to greater foam expansion and a lower foam density. However, a slight reduction in compressive modulus was observed with 2 pbw surfactant loading, after which the modulus stabilized (Figure 6c). Thirumal et al. [3] linked stress-strain behaviour to hardness and toughness, noting that higher foam density typically results in greater resistance to indentation and a higher compressive modulus. This trend was observed at low surfactant levels, where higher-density foam exhibited a higher compressive modulus. However, as surfactant content increased, the foam density decreased, leading to a reduction in compressive strength. Seo et al. [31] also found that increased surfactant content reduced mechanical strength due to its plasticizing effects.

Water Absorption

The percentage of water absorption increased with the introduction of residue in the foam formulation (Figure 7a), rising from 91 % (without residue) to 122 % (with residue). This increase can be attributed to the hydrophilic nature of the AM polyol residue. Wood particles, which contain free hydroxyl (OH) groups from cellulose and hemicellulose, can form hydrogen bonds with water, resulting in weight gain [32]. Additionally, the weak interfacial adhesion between the AM polyol residue and the foam’s membrane cells may facilitate greater bonding with water. This is because moisture content is largely influenced by the amorphous regions and voids in the material.

The percentage of water uptake significantly decreased with the addition of 3 pbw of water, after which it slightly increased (Figure 7b). The high blowing capacity at elevated water loadings may cause the residue to detach from the foam membrane, leading to cell breakage. The resulting voids facilitate greater water absorption. Additionally, the split residues may form hydrogen bonds with water, contributing to higher weight gains at 4 pbw water loading.

Water uptake initially increased slightly before decreasing significantly after the addition of 3 pbw of surfactant (Figure 7c). This reduction may be attributed to the siloxane component in the surfactant, which has hydrophobic characteristics that inhibit water absorption in foam [1].

Dynamic Mechanical Analysis (DMA)

Figure 8a illustrates the storage modulus and tan δ of AMPU foams with and without residue. The glass transition temperature (Tg) exhibited a shoulder around 80–110 ºC due to the AM polyol residue, which was not present in foams without residue. The Tg shifted significantly from 147 ºC (without residue) to 191 ºC (with residue), suggesting that isocyanate reacted with both the hydroxyl groups and moisture from the wood, forming strong PU linkages [28]. This shift in Tg indicated improved hardness in the rubbery modulus.

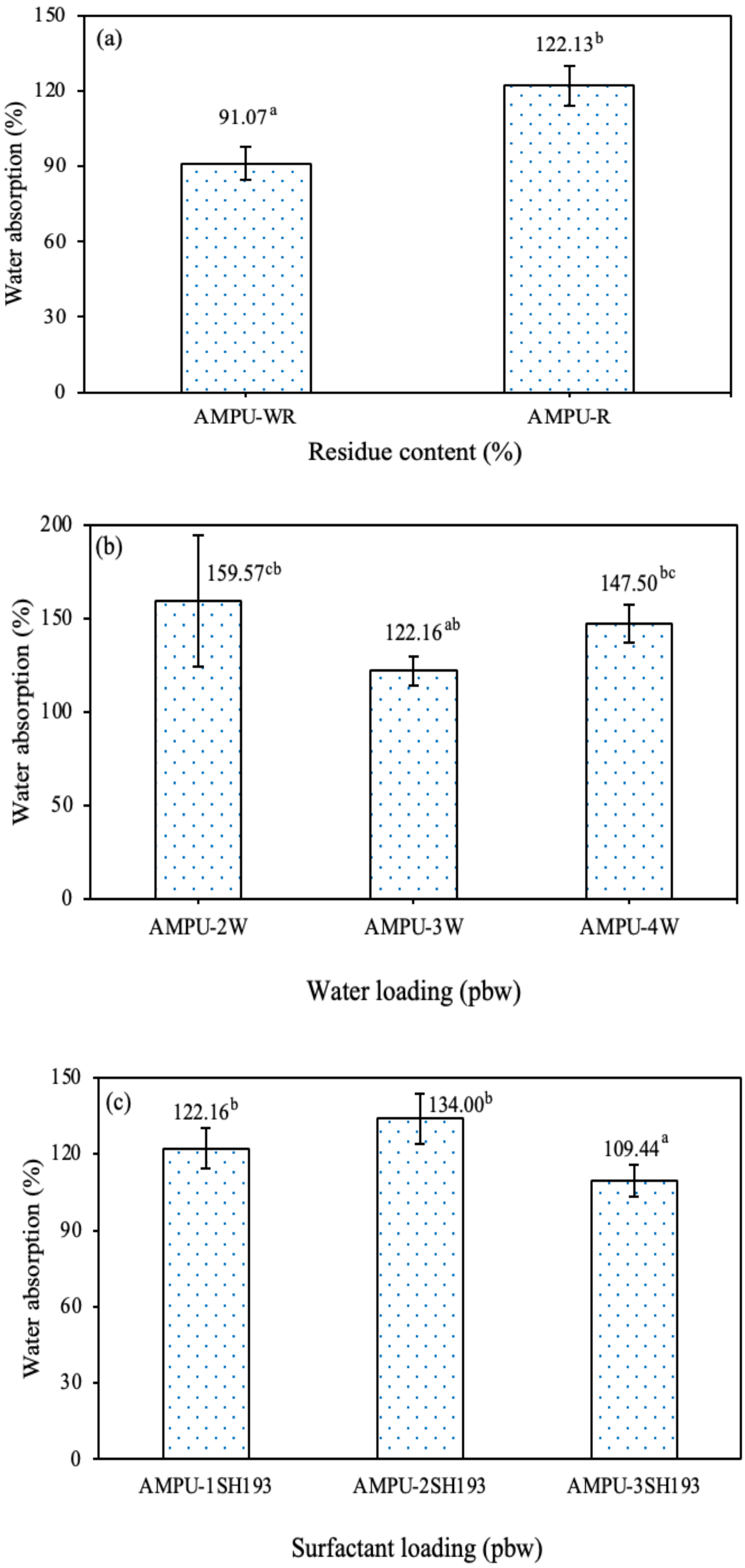

Figure 7. Water absorption of AMPU foam: (a) with residue (AMPU-R) and without residue (AMPU-WR), (b) with different water loadings, (c) with different surfactant loadings.

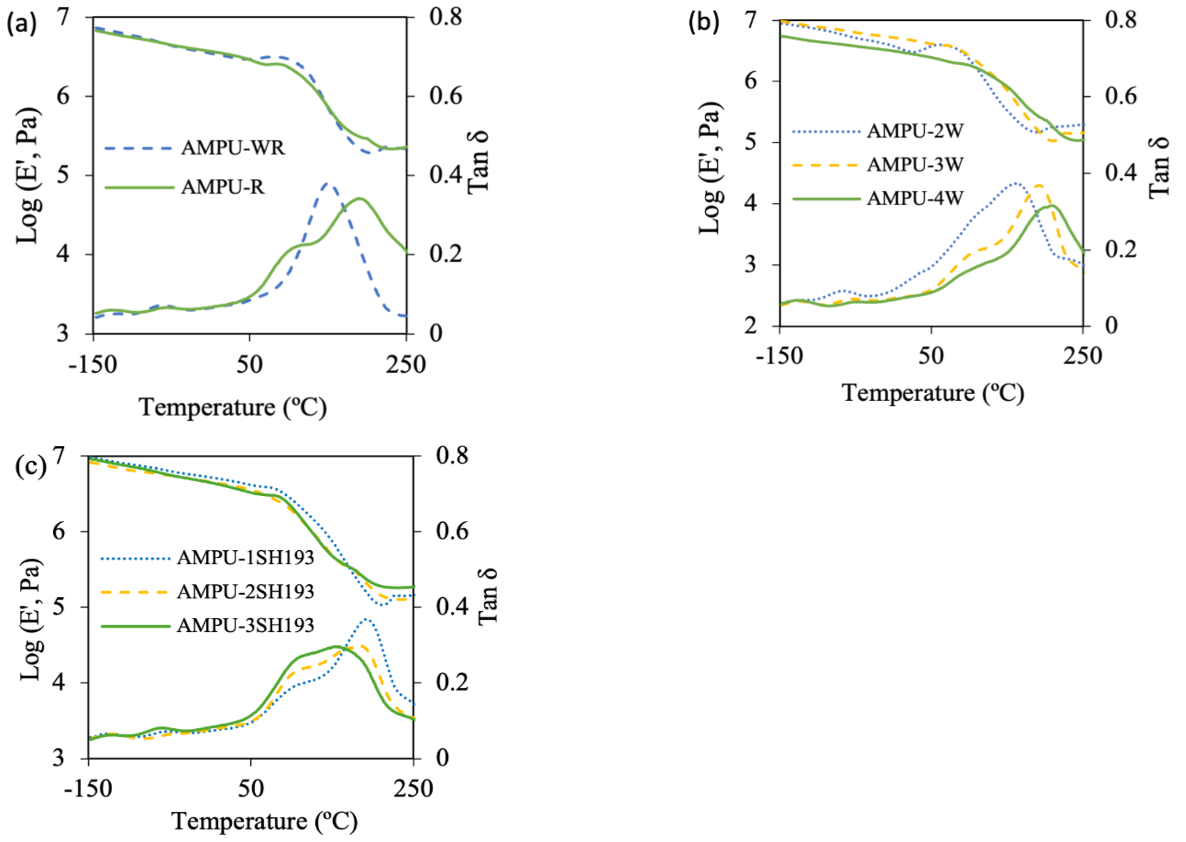

Figure 8. Storage modulus and tan δ of AMPU foams: (a) with residue (AMPU-R) and without residue (AMPU-WR), (b) with different water loadings, (c) with different surfactant loadings.

Increasing water loading also impacted the viscoelastic behaviour of AMPU foams (Figure 8b), with Tg increasing linearly as water loading increased. This trend is likely linked to the formation of rigid urea bonds (1660 cm^{-1}) that were observed in the FTIR and 2D-COS analyses. The increased rigidity led to a higher Tg, reflecting enhanced crosslinking density. Conversely, Tg decreased significantly with higher surfactant loadings (Figure 8c). Similar results have been reported by Seo et al. [31], where Tg decreased as surfactant levels rose, indicating that surfactants may act as plasticizers in the foam matrix.

CONCLUSION

This study demonstrates that incorporating *Acacia mangium* polyol residue resulted in higher foam density and increased crosslinking density, although it also led to reduced elasticity. The hydrophilic nature of the AM polyol residue significantly contributed to the foam's high water absorption. Additionally, both the increased water loading and surfactant content profoundly affected the mechanical properties of the foam. Notably, the elevated formation of urea, indicated by the absorbance peak at 1660 cm^{-1} in the FT-IR spectrum, correlated with the enhanced rigidity of the AMPU foam and its high crosslinking density. The presence of larger, thinner cells at higher water and surfactant levels further suggests a reduction in density, which compromised the elasticity of the AMPU foam. These findings contribute to the growing field of bio-based polyurethane foams by demonstrating the potential for utilizing sustainable, renewable materials in foam production. The ability to tailor foam properties through the manipulation of water and surfactant content, along with the inclusion of wood residues, opens the door to more eco-friendly alternatives to traditional petrochemical-based foams. Furthermore, the improved mechanical properties, such as increased crosslinking density and rigidity, could be particularly valuable in applications requiring enhanced strength and durability. While further research is needed to optimize elasticity, the insights gained from this study provide a foundation for the large-scale production of bio-based polyurethane foams with diverse applications in industries such as construction, automotive, and packaging.

REFERENCES

1. Lim, H., Kim, S. H. and Kim, B. K. (2008) Effects of silicone surfactant in rigid polyurethane

foams. *eXPRESS Polymer Letters*, **2(3)**, 194-200. DOI:10.3144/expresspolymlett.2008.24.

2. Kim, S. H. and Kim, B. K. (2008) Effect of isocyanate index on the properties of rigid polyurethane foams blown by HFC 365mfc. *Macromolecular Research*, **16(5)**, 467–472. DOI:10.1007/BF03218546.
3. Thirumal, M., Khastgir, D., Singha, N. K., Manjunath, B. S. and Naik Y. P. (2008) Effect of foam density on the properties of water blown rigid polyurethane foam. *Journal of Applied Polymer Science*, **108(3)**, 1810-1817. https://doi.org/10.1002/app.27712.
4. Yao, Y., Yoshioka, M. and Shiraishi, N. (1996) Water-absorbing polyurethane foams from liquefied starch, *Journal of Applied Polymer Science*, **60(11)**, 1939–1949.
5. Maldas, D. and Shiraishi, N. (1996) Liquefaction of wood in the presence of polyol using NaOH as a catalyst and its application to polyurethane foams. *International journal of Polymeric Materials and Polymeric Biomaterials*, **33(1-2)**. https://doi.org/10.1080/00914039608028608.
6. Zhang, J., Hori, N. and Takemura, A. (2022) Stability and degradation of four agricultural wastes liquefied polyols based polyurethane foams. *Journal of Applied Polymer Science*, **139(37)**, e52893.
7. Mosiewicki, M. A., Dell'Arciprete, G. A., Aranguren, M. I. and Marcovich, N. E. (2009) Polyurethane foams obtained from castor oil-based polyol and filled with wood flour. *Journal of Composite Materials*, **43(25)**. DOI:10.1177/0021998309345342.
8. Luo, S., Gao, L. and Guo, W. (2020) Influence of Adding Lignin and Wood as Reactive Fillers on the Properties of Lightweight Wood–Polyurethane Composite Foams. *Forest Products Journal*, **70(4)**, 420–427.
9. Fauzi, F. N. A. M., Bonnia, N. N., Setik, R., Anuar, A. U., Rahman, Z. A., Hizrin, R. S. F. N., Affandi, N. D. N. (2024) Physical and morphological analysis of polyurethane with different ratios of polyol & isocyanate for grouting applications. *Malaysian Journal of Chemistry*, **26(6)**, 46–57.
10. Palle, I., Lodin, V., Mohd Yunus, A. M., Lee, S. H., Paridah, M. T., Hori, N., Antov, P. and Takemura, A. (2023) Effects of NCO/OH ratios on bio-based polyurethane film properties made from *Acacia mangium* liquefied wood. *Polymers*, **15(5)**, 1154. https://doi.org/10.3390/polym15051154
11. Palle, I., Hori, N., Iwata, T. and Takemura, A. (2018) Optimization of polyol production via liquefaction from *Acacia mangium* and analysis of the polyols by traditional methods and two-dimensional correlation spectroscopy. *Holzforschung*, **72(6)**, 451. https://doi.org/10.1515/ hf-2017-0076.
12. Uram, K., Kurańska, M., Andrzejewski, J. and Prociak, A. (2021) Rigid polyurethane foams modified with biochar. *Materials*, **14(19)**, 5616.
13. Członka, S., Strąkowska, A. and Kairytė, A. (2021) Coir fibers treated with henna as a potential reinforcing filler in the synthesis of polyurethane composites. *Materials*, **14(5)**, 1128.
14. Kurimoto, Y., Takeda, M., Doi, S., Tamura, Y. and Ono, H. (2001) Network structures and thermal properties of polyurethane films prepared from liquefied wood. *Bioresource Technology*, **77(1)**, 33-40. https://doi.org/10.1016/S0960-8524(00)00136-X.
15. Teo, L. S., Chen, C. Y. and Kuo, J. F. (1997) Fourier transform infrared spectroscopy study on effects of temperature on hydrogen bonding in amine-containing polyurethanes and poly(urethane-urea)s. *Macromolecules*, **30(6)**, 1793–1799. https://doi.org/10.1021/ma961035f.
16. Yilgor, I., Yilgor, E., Guler, I. G., Ward, T. C. and Wilkes, G. L. (2006) FTIR investigation of the influence of diisocyanate symmetry on the morphology development in model segmented polyurethanes. *Polymers*, **47(11)**, 4105–4114. https://doi.org/10.1016/j.polymer.2006.02.027.
17. Abd Hilmi, N. H., Lodin, V., Gilbert Jesuet, M. S., Salim, S., Lee, S. H., Hori, N., Takemura, A. and Palle, I. (2023) Producing *Eucalyptus pellita* wood polyol through liquefaction for polyurethane film production. *Industrial Crops and Products*, **205**, 117431. https://doi.org/10.1016/j.indcrop.2023.117431.
18. Fuensanta, M. and Martin-Martinez, J. M. (2020) Viscoelastic and adhesion properties of new poly (ether-urethane) pressure sensitive adhesives. *Frontiers in Mechanical Engineering*, **6**. https://doi.org/10.3389/fmech.2020.00034.
19. Coleman, M. M., Lee, K. H., Skrovanek, D. J. and Painter, P. C. (1988) Hydrogen bonding in polymer blends. 1. FTIR studies of urethane-ether blends. *Macromolecules*, **21(1)**, 59-65. https://doi.org/10.1021/ma00179a014.
20. Noda, I. (2014) Frontiers of two-dimensional correlation spectroscopy. Part I. New concepts and noteworthy developments. *Journal of Molecular*

Structure, **1069**, 3-22. https://doi.org/10.1016/j.molstruc.2014.01.025.

21. Szycher, M. (2013) Szycher's handbook of polyurethanes, Second edition. *CRC Press NY.*

22. Rodrigue, D., Souici, S. and Twite-Kabamba, E. (2006) Effect of wood powder on polymer foam nucleation. *Journal of Vinyl and Additive Technology*, **12(1)**, 19–24. https://doi.org/10.1002/vnl.20062.

23. Prociak, A., Malewska, E., Bak, S. (2015) Influence of isocyanate index on selected properties of flexible polyurethane foams modified with various bio-components. *Journal of Renewable Materials*, **4(1)**, 78–85. DOI: 10.7569/JRM.2015.634129.

24. Niyogi, D., Kumar, R. and Gandhi, K. S. (2004) Water blown fee rise polyurethane foam. *Polymer Engineering and Science*, **39(1)**, 199–209. https://doi.org/10.1002/pen.11408.

25. Dukarska, D., Walkiewicz, J., Derkowski, A. and Mirski, R. (2022) Properties of rigid polyurethane foam filled with sawdust from primary wood processing. *Materials*, **15(15)**, 5361.

26. Han, M. S., Choi, S. J., Kim, J. M., Kim, Y. H. and Kim, W. N. (2009) Effects of silicone surfactant on the cell size and thermal conductivity of rigid polyurethane foams by environmentally friendly blowing agents. *Macromolecular Research*, **17**, 44-50. https://doi.org/10.1007/bf03218600.

27. Borreguero, A. M., Rodriguez, J. F., Valverde, J. L., Arevalo, R., Peijs, T. and Carmona, M. (2011) Characterization of rigid polyurethane foams containing microencapsulated Rubitherm®RT27: catalyst effect. Part II. *Journal of Material Sciences*, **46(2)**, 347.

28. Yuan, J. and Shi, S. Q. (2009) Effect of the addition on wood flours on the properties of rigid polyurethane foam. *Journal of Applied Polymer Science*, **113(5)**, 2902. DOI:10.1002/app.30322.

29. Krishnamurti, B., Bharadwaj-Somaskandan, S., Sergeeva, T. and Shutov, F. (2003) Effect of wood flour fillers on density and mechanical properties of polyurethane foams. *Cell Polym.*, **22(6)**, 371–382.

30. Goods, S. H., Neuschwanger, C. L., Henderson, C. C. and Skala, D. M. (1998) Mechanical properties of CRETE, a polyurethane foam. *Journal of Applied Polymer Science*, **68(7)**, 1045–1055.

31. Seo, W. J., Jung, H. C., Hyun, J. C., Kim, W. N., Lee, Y. B., Choe, K. H., Kim, S. B. (2003) Mechanical, morphological and thermal properties of rigid polyurethane foams blown by distilled water. *Journal of Applied Polymer Science*, **90(1)**, 12–21. https://doi.org/10.1002/app.12238.

32. Mohd Idrus, M. A. M., Hamdan, S., Rahman, M. R. and Islam, M. S. (2011) Treated tropical wood sawdust-polypropylene polymer composite: Mechanical and morphological study. *Journal of Biomaterials and Nanobiotechnology*, **2(4)**. DOI:10.4236/jbnb.2011.24053.